Geotextiles and Geomembranes 26 (2008) 488–497

Contents lists available at ScienceDirect

Geotextiles and Geomembranes

journal homepage: www.elsevier.com/locate/geotexmem

Geomembrane strains from coarse gravel and wrinkles in a GM/GCL composite liner

R.W.I. Brachman*, S. Gudina

GeoEngineering Centre at Queen's–RMC, Queen's University, Kingston, Ontario K7L 4P5, Canada

ARTICLE INFO

Article history:
Received 14 September 2007
Received in revised form 29 April 2008
Accepted 4 May 2008
Available online 20 June 2008

Keywords:
Geomembrane
Geosynthetic clay liner
Wrinkle
Landfill
Liner protection

ABSTRACT

The physical response of a 1.5-mm-thick, high-density polyethylene geomembrane (GM) is reported when placed on top of a needle-punched geosynthetic clay liner (GCL), buried beneath 50-mm coarse gravel and subjected to vertical pressure in laboratory experiments. Local strains in the geomembrane caused by indentations from the overlying gravel and deflections of a wrinkle in the geomembrane are quantified. A peak strain of 20% was calculated when a flat geomembrane was tested without a protection layer at an applied vertical pressure of 250 kPa. Strains were smaller with a nonwoven needle-punched geotextile protection layer between the gravel and geomembrane. Increasing the mass per unit area of the geotextile up to 2200 g/m^2 reduced the geomembrane strain. However, none of the geotextiles tested were sufficient to reduce the geomembrane strain below an allowable limit of 3%, for the particular 50-mm gravel tested and when subjected to a vertical pressure of 250 kPa. Increasing the initial GCL water content and reducing the stiffness of the foundation layer beneath the GCL were found to increase the geomembrane strains. These local strains were greater when a wrinkle was present in the geomembrane. The wrinkle in the geomembrane experienced a decrease in height and width. The wrinkle deformations lead to larger pressures beside the wrinkle and hence producing larger local strains. A 150-mm-thick sand protection layer was effective in limiting the peak strain to less than 0.3% even with a wrinkle in the geomembrane, at a vertical pressure of 250 kPa.

1. Introduction

Composite liner systems consisting of a geomembrane (GM) over a geosynthetic clay liner (GCL), Fig. 1, can be an effective barrier to contaminant transport in a solid waste landfill (e.g., Rowe et al., 2004, 2007; Rowe, 2005; Barroso et al., 2006; Dickinson and Brachman, 2006; Touze-Foltz et al., 2006; Bouazza and Vangpaisal, 2006; Bouazza et al., 2008; Saidi et al., 2008). To act as an effective barrier, physical damage to the geomembrane and GCL must be limited to allowable levels. Consequently, a protection layer is required above the GM/GCL to: prevent geomembrane puncture during placement of the overlying drainage material and waste (Koerner et al., 1996), limit the long-term geomembrane tensile strains that may over time lead to stress-cracking and development of holes in the geomembrane (Rowe et al., 2004), and reduce local thinning of the GCL from extrusion of bentonite (Fox et al., 2000).

The physical conditions experienced by the GM/GCL are exacerbated by using coarse gravel in the overlying leachate collection system (to minimize biologically induced clogging; Fleming and Rowe, 2004), resulting in larger and more widely spaced contact forces on the geomembrane (and hence larger strains) relative to finer gravel or sand. Wrinkles (e.g., see Fig. 1b) that form in the geomembrane during installation from solar heating and/or placement of overlying materials also influence the physical conditions experienced by the liner. The wrinkle causes a redistribution of vertical stresses acting on the liner with zero stresses directly beneath the wrinkle and increased stresses on both sides of the wrinkle. Deformation of the wrinkle when buried may also lead to changes in tensile strain in the geomembrane.

The physical response of the geomembrane when part of a composite liner with compacted clay has been previously quantified. For example, Tognon et al. (2000) have reported strains in a high-density polyethylene geomembrane overlying a compacted clay liner, buried beneath coarse gravel backfill and subjected to applied vertical pressure. While the geomembrane was not punctured, its long-term tensile strains exceeded the 6% allowable long-term strain criterion (for smooth materials with a stress crack resistance less than 1500 h proposed by Peggs et al., 2005) when a conventional nonwoven, needle-punched geotextile (mass per unit area of 435 g/m^2) was used as the protection layer (at an applied pressure of 250 kPa). By testing similar materials Gudina and Brachman (2006a) showed these local geomembrane strains were even larger when the geomembrane was wrinkled. Also,

* Corresponding author. Tel.: +1 613 533 3096; fax: +1 613 533 2128.
E-mail address: brachman@civil.queensu.ca (R.W.I. Brachman).

0266-1144/$ – see front matter © 2008 Elsevier Ltd. All rights reserved.
doi:10.1016/j.geotexmem.2008.05.001

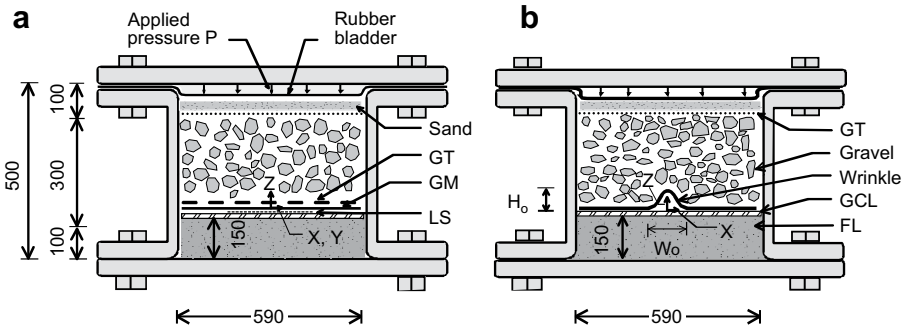

Fig. 1. Cross-section through test cell: (a) geomembrane without a wrinkle and (b) wrinkled geomembrane. Dimensions in millimetres. GM = geomembrane, GT = geotextile, LS = lead sheet, GCL = geosynthetic clay liner, FL = foundation layer; *X*, *Y* and *Z* are Cartesian coordinates; and H_o and W_o = initial height and width of wrinkle, respectively.

Soong and Koerner (1998) measured geomembrane wrinkle deformations for the specific case with sand above and below the geomembrane. Their results showed that although the wrinkle experienced a decrease in height and width, the gap beneath the wrinkle remained even when subjected to a pressure of up to 1100 kPa and test duration of 1000 h. When compacted clay was tested beneath the geomembrane, Gudina and Brachman (2006a) observed a different response where the gap beneath the wrinkle was completely filled with clay, depending on the applied pressure and the clay water content.

There is a paucity of data on the physical response of the geomembrane when it is part of a composite liner with a GCL. Dickinson and Brachman (2006) have reported how the GCL can become thinner for a GM/GCL liner with a wrinkle and beneath coarse gravel. They found that the thickness of the GCL decreased beside the wrinkle and increased beneath the wrinkle from bentonite extrusion towards the gap beneath the wrinkle. The gravel backfill above the geomembrane was observed to cause large variations in the thickness of the GCL, caused by bentonite extrusion directly beneath gravel contacts to zones in between contacts. They also found that this extrusion was exacerbated by the presence of the wrinkle as it increased the vertical stresses adjacent to the wrinkle.

However, Dickinson and Brachman (2006) focussed exclusively on the physical response of the GCL. It is the objective of this paper to report measured geomembrane deformations and strains of a GM/GCL composite liner (1.5-mm-thick high-density polyethylene GM on top of a needle-punched GCL) when buried beneath coarse gravel from physical tests. Geomembrane strains are reported for tests conducted with and without a wrinkle. The influence of protection layer, GCL water content and subgrade beneath the GCL on local geomembrane strains and wrinkle deformations are examined.

2. Experimental details

2.1. Test cell

Fig. 1 shows a cross-section through the test cell, which is a cylindrical steel pressure vessel with an inside diameter of 590 mm and a height of 500 mm. Vertical overburden pressures are simulated by applying water pressure to a rubber bladder along the top surface of the soil. The test cell was designed to limit the outward deflection of the sidewalls to produce horizontal stresses corresponding to zero lateral strain conditions. To minimize boundary friction, the sidewalls of the test cell were treated with two layers of 0.1-mm-thick polyethylene (PE) sheets lubricated with a high-temperature bearing grease (Gudina, 2007). This friction treatment reduces the sidewall friction angle to less than 5° (Tognon et al., 1999). For the size of the test cell and the friction treatment employed, the pressure loss due to boundary friction at the location of the geomembrane is calculated to be less than 5% (Brachman and Gudina, 2002). Since the effect of boundary friction is minimized, but not eliminated, the reported values of applied pressure should be reduced by 5% when considering an equivalent burial depth in a landfill.

Fig. 1 also shows the coordinate system for the geomembrane. The coordinate $X = 0$, $Y = 0$ represents the centre of the test cell and $Z = 0$ is at the initial elevation of the geomembrane.

2.2. Materials tested

A summary of the configurations tested are given in Tables 1 and 2 for tests without (Tests 1–8) and with (Tests 9–17) a wrinkle in the geomembrane. The foundation layer beneath the GM/GCL liner in Tests 1–7 and 9–15 was a 150-mm-thick layer of dry, poorly graded medium-sand (SP), to simulate the case of a firm foundation layer beneath the GCL. This sand had a mean grain size of 0.45 mm, uniformity coefficient of 2.7 and coefficient of curvature of 0.7. It was installed at a dry density of 1.91 g/cm^3 corresponding to a density index of 85% and had water content of less than 0.2%. To investigate the influence of a much softer foundation layer, a 150-mm-thick compacted clay foundation layer (CCL) was used in Tests 8, 16, and 17. This foundation layer was constructed using a silty clay (CL) soil that was obtained from a landfill site in Milton, Ontario, Canada. It had a liquid limit of 26%, a plastic limit of 16%, a grain size with 32% finer by mass than 2 μm, and standard Proctor optimum water content of 12% at a maximum dry density of 2.1 g/cm^3. The clay was placed and compacted at a water content of 16%, which is the likely upper limit on moulding water content to produce a good quality clay liner (Benson et al., 1999), and had an average dry density of 1.9 g/cm^3.

The particular GCL tested consisted of sodium bentonite (4721 g/m^2) between a slit-film woven carrier geotextile (110 g/m^2) and a virgin staple fibre nonwoven cover geotextile (241 g/m^2). It

Table 1
Summary of tests with a flat geomembrane (no wrinkle)

	Foundation layer	Protection layer	GCL water content (%)	Peak GM strain (%)
1	SP	None	7	13
2	SP	None	128	17
3	SP	None	170	20
4	SP	GT1	129	10
5	SP	GT2	128	7.7
6	SP	GT3	148	5.5
7	SP	SP	126	0.2
8a	CCL	None	7	20
8b	CCL	None	7	22

Table 2
Summary of tests with a wrinkle in the geomembrane

Test	Test conditions				Peak GM strain beside a wrinkle (%)
	Foundation layer	Protection layer	H_o (mm)	GCL water content (%)	
9a	SP	None	63.4	7	–
9b	SP	None	59.6	7	–
9c	SP	None	60.6	7	14
10a	SP	None	61.0	126	12
10b	SP	None	67.0	140	14
10c	SP	None	62.5	139	18
11a	SP	None	63.2	184	17
11b	SP	None	62.6	173	22
12a	SP	GT2	66.2	113	9.6
12b	SP	GT2	64.0	121	8.8
12c	SP	GT2	64.7	127	9.9
13	SP	GT3	63.3	115	7.5
14a	SP	SP	64.4	128	0.3
14b	SP	SP	62.3	121	0.3
14c	SP	SP	62.9	135	0.3
15	SP	SP	60.0	138	0.4
16	CCL	None	64.2	7	21
17	CCL	None	66.0	148	31

was needle-punched and the needle-punched fibres were thermally fused to the carrier geotextile. The GCL was installed with the woven geotextile facing down. The response of the composite liner was examined for three different GCL water contents. For Tests 1, 8, 9, and 16 the GCL was tested dry without hydration and had an average initial gravimetric water content of 7%. The dry GCL had an average thickness of 5.5 ± 0.2 mm (where ± 0.2 is the 95% confidence interval of the mean) and was obtained from over 1300 measurements per specimen (Dickinson and Brachman, 2006). For Tests 2, 4–7 and 10–16 the GCL was hydrated for 14 days under a confining stress of 20 kPa. This resulted in an average thickness of 7.7 ± 0.3 mm and initial water contents between 113 and 148%. In Tests 3, 11 and 17, the GCL was hydrated for 14 days without any confining stress. The average thickness of these GCLs was 10.5 ± 1.0 mm with initial water contents between 148 and 184%.

In all tests, a 1.5-mm-thick smooth high-density polyethylene geomembrane was placed above the GCL. Tensile stress–strain properties of the geomembrane tested are given in Table 3. In Tests 1–8, a flat geomembrane (i.e., without a wrinkle) was tested. In these tests, a 0.4-mm-thick lead sheet (270 mm wide $\times$ 270 mm long) was installed between the geomembrane and the GCL at the centre of the test cell to measure the local geomembrane deformations. In Tests 9–17, a wrinkle was artificially formed in the geomembrane with an initial target height H_o of 60 mm and width W_o of 240 mm (Fig. 1b). The geometry of the initial wrinkle was measured to an accuracy of ± 0.1 mm using a profiler consisting of a series of displacement transducers mounted on a linear rail. A wrinkle with these dimensions lies within the range of available field observations reported by Pelte et al. (1994).

Table 3
Stress–strain properties (mean $\pm$ 95% confidence interval) of the particular geomembrane tested

Property	Machine direction	Cross-machine direction	Average (machine and cross-machine)
Yield strength, σ_Y (kN/m)	30 ± 0.8	32 ± 0.6	31 ± 0.8
Break yield strength, σ_B (kN/m)	50 ± 4	58 ± 3	53 ± 4
Yield elongation strain, ε_Y (%)	20 ± 0.3	18 ± 0.1	19 ± 0.6
Break elongation strain, ε_B (%)	810 ± 80	960 ± 50	885 ± 70
2% Secant modulus, $E_{2\%}$ (MPa)	270 ± 13	320 ± 21	295 ± 20

Obtained from five tests in each direction following ASTM D 5323 and D 6693 (ASTM 1992, 2001).

The type of protection layer between the geomembrane and the overlying coarse gravel drainage layer is listed in Tables 1 and 2. The tests conducted with no protection layer serve as a baseline for comparison with tests where protection was used. Three nonwoven needle-punched geotextiles with masses per unit area equal to 390, 1200 and 2200 g/m^2, denoted as GT1, GT2 and GT3, respectively, were investigated. A protection layer consisting of a 150-mm-thick layer of poorly graded sand (SP) was also tested. This was the same sand as that used for the foundation layer, but was placed without compaction at a density of 1.75 g/cm^3 (density index of 30%). The sand was placed directly on top of the geomembrane. A nonwoven needle-punched geotextile (390 g/m^2) was used to separate the sand from the overlying coarse gravel.

A 300-mm-thick layer of nominal 50-mm poorly graded coarse gravel (GP) meeting the requirements of Ontario, Canada landfill regulations (MOE, 1998) was placed above the geomembrane to simulate a granular leachate collection system. The gravel was obtained from crushed limestone and as a result, the gravel particles were rough and angular. The particle gradation varied between 19 and 75 mm with a mean particle size of approximately 50 mm. It was placed without compaction at a dry density of 1.5 g/cm^3.

2.3. Liner boundary conditions

For the tests conducted with no wrinkle, the geomembrane specimen was cut to tightly fit up against the test cell walls providing a zero radial deflection boundary. The boundary conditions for the geomembrane liner are more complex for tests involving a wrinkle. First, a 5-mm wide gap was intentionally left between the ends of the geomembrane wrinkle and the test cell wall (i.e., at $Y = \pm 295$ mm) to prevent binding of the geomembrane against the test cell wall. This was successful in providing a reproducible zero stress boundary condition at the ends of the wrinkle. Three-dimensional finite element analysis (Brachman and Gudina, 2002) has shown that this boundary condition results in negligible effects (<0.1% difference in vertical deflection) relative to axial plane strain conditions (those expected to prevail for a long wrinkle in the field) for the central 120 mm of the test specimen, for which all results were reported. Second, perpendicular to the wrinkle at either end of the geomembrane ($X = \pm 295$ mm) possible lateral deflection of the geomembrane (i.e., outward translation of the geomembrane along the GM/GCL interface) was prevented by casting small plaster blocks between the geomembrane and the test cell wall. Gudina and Brachman (2006b) showed that lack of lateral restraint can lead to displacement of the geomembrane at the GM/GCL interface and hence can lead to larger wrinkle deformations. They further showed that lateral displacement was most prominent (up to 16 mm) when the GCL had large initial water content. Since such displacements are not expected at the base of a landfill with laterally extensive conditions, providing lateral restraint is important to obtain a more realistic simulation of field conditions in these experiments.

2.4. Test procedure

Once the materials were placed in the test cell, the bladder was installed. This consisted of a 3-mm-thick gum rubber bladder clamped between the flange and lid of the test cell. A separator geotextile and a 50-mm-thick layer of sand were used to protect the bladder from possible damage from the gravel. All tests (except Test

15) were conducted at an applied pressure of 250 kPa, applied in increments of 50 kPa every 10 min until the maximum test pressure was reached. Test 15 was conducted at an applied pressure of 1000 kPa (using increments of 100 kPa every 10 min) to investigate the influence of a larger pressure on the wrinkle. An applied pressure of 250 kPa corresponds to burial under approximately 18 m of waste (assuming a unit weight of waste of 13 kN/m^3 and accounting for 5% loss in applied pressure from boundary friction). The maximum pressure was maintained for 10 h. All tests were conducted at a temperature of 22 ± 1 °C.

At the end of each test, the pressure was released and the drainage material was carefully removed. The geomembrane was visually inspected for any possible damage, scratches or permanent deformations. For tests without a wrinkle, a mould of the lead sheet was then cast with low-shrinkage plaster of Paris to preserve its deformed shape. After the mould had set, it was removed from the test cell and then five most prominent indentations were selected for the assessment of strain. These indentations were then scanned along two perpendicular axes by a laser scanner with a measurement accuracy of ± 0.05 mm.

For tests with a wrinkle, at the end of the 10-h test duration and while the pressure was still being applied, a low-shrinkage grout made from the same plaster of Paris was injected into any remaining gap beneath the geomembrane to preserve the final geometry of the gap beneath the geomembrane wrinkle. The final height and width of the wrinkle were measured to accuracies of ± 0.1 and ± 5 mm, respectively, using the profiler.

3. Results

3.1. Local strain in flat geomembranes

The geomembrane was not punctured in any of the tests reported in this paper. The calculated peak tensile strains in the geomembrane are given in Table 1. These strains were calculated from the measured geomembrane indentations in the lead sheet using the method of Tognon et al. (2000), considering both membrane and bending strains and taking tensile strains as positive.

The geomembrane strain was found to vary based on the size of the indentation, with narrower and deeper indentations producing the largest strains. For example, the deformed shape of the indentations producing the largest strain in each of Tests 2 and 6 is plotted in Figs. 2 and 3 (where h is the vertical distance above the deepest point of the indentation). The components of membrane (ε_m) and bending (ε_b) strain, and the resulting strain distributions for the top and bottom surface of the geomembrane (ε_{top} and ε_{bot}) are also given. Fig. 2b shows that membrane strains increase from zero at the deepest point to a maximum roughly half-way up the indentation, while the magnitude of the bending strains are largest at the deepest point and near the top of the indentation and change sign roughly half-way up the indentation. The largest overall tensile strain generally occurred on the bottom surface located roughly half-way up the indentation as a result of membrane strain combined with some bending. For example in Test 2, a peak strain of 17% occurred 4 mm away from the deepest point of the indentation (Fig. 2c), whereas a peak strain of 5.5% was found −6 mm from the deepest point in Test 6 (Fig. 3c).

Comparing the results of Tests 1–3 in Table 1 shows that as the GCL water content was increased, the peak tensile strain increased. This is attributed to the decrease in shear strength and stiffness of the GCL with increasing water content.

The effectiveness of the protection layers tested at reducing geomembrane strains is plotted in Fig. 4. Calculated strains from the five most significant indentations are plotted from each test. These results were all obtained with the GCL hydrated under confining stress (initial GCL water contents ranging from 128 to 148%).

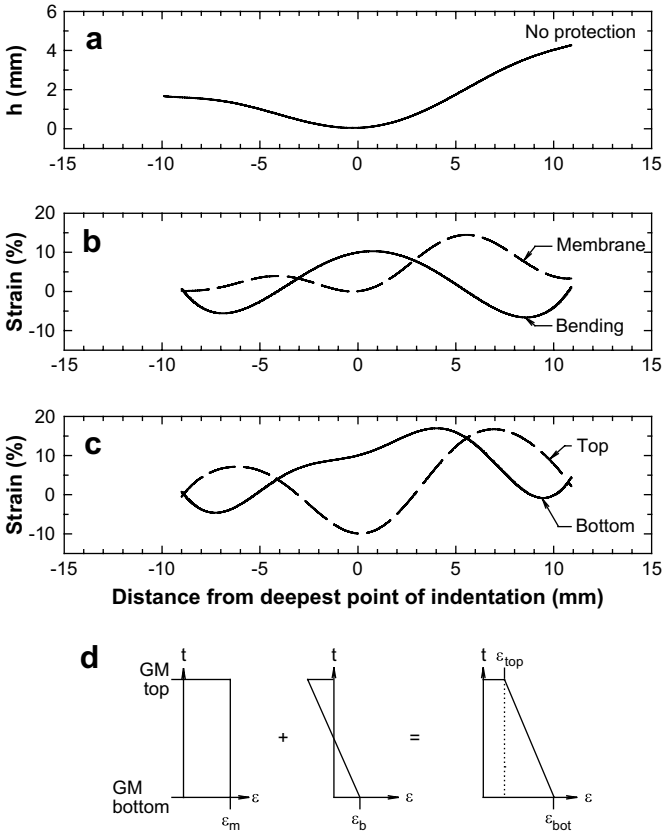

Fig. 2. Local indentation and strains in GM from Test 2 with no protection: (a) deformed shape, (b) membrane and bending strains, (c) bottom and top strains, and (d) schematic of strain components through the GM thickness (t).

The results in Fig. 4 show that geomembranes' strains with a nonwoven needle-punched geotextile are less than those with no protection, and that increasing the mass per unit area of the geotextile reduces the strain. However, the maximum tensile strain with either GT1 or GT2 exceed the limit of 6% proposed by Peggs

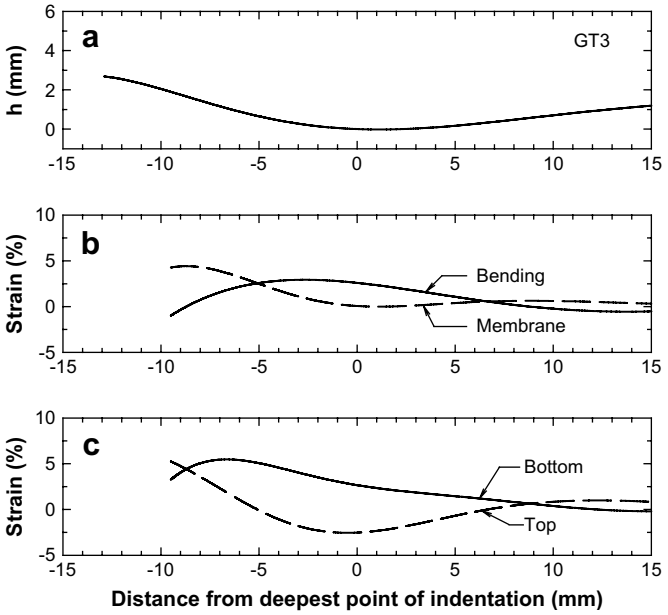

Fig. 3. Local indentation and strains in GM from Test 6 protected with GT3: (a) deformed shape, (b) membrane and bending strains, and (c) bottom and top strains.

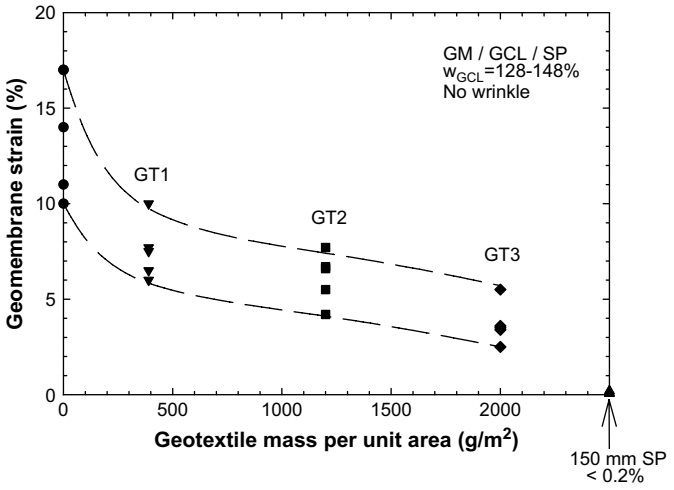

Fig. 4. Effectiveness of protection layers at reducing geomembrane strains.

et al. (2005) and consequently they should not be relied upon to limit geomembrane strains for the 50-mm gravel tested when loaded to 250 kPa. While the very thick GT3 resulted in short-term strains just less than 6%, even this product is not recommended for pressures of 250 kPa. This is because the tests conducted do not attempt to account for the long-time frames, elevated temperatures and chemical exposure that are expected to occur under field conditions in a landfill. Additional strain from geotextile creep and softening at higher temperatures may be expected to result in geomembrane strains greater than 6%. That the nonwoven needle-punched geotextiles were able to prevent puncture but unable to limit the tensile strains is consistent with the observations from Tognon et al. (2000) and Gudina and Brachman (2006a), both for the case of compacted clay beneath the geomembrane (i.e., no GCL). The inability of the nonwoven geotextiles to limit strains to small levels is from initial slack in their stress–strain response as the needle-punched fibres are stretched and engaged (initial tangent offsets up to 20% strain in wide-width tension tests). The deformation required to overcome this slack and fully mobilize their stiffness has already contributed to geomembrane strain.

The 150-mm-thick sand layer was the most effective, limiting the maximum tensile strain to less than 0.2% (see Table 1 and Fig. 4). Of the protection layers tested, only the sand layer limited strains to the more restrictive allowable long-term strain of 3% required by German landfill standards (Seeger and Müller, 2003). Another advantage of sand is that, unlike geosynthetic protection layers, issues of a finite service life and long-term creep of the protection layer do not come into play.

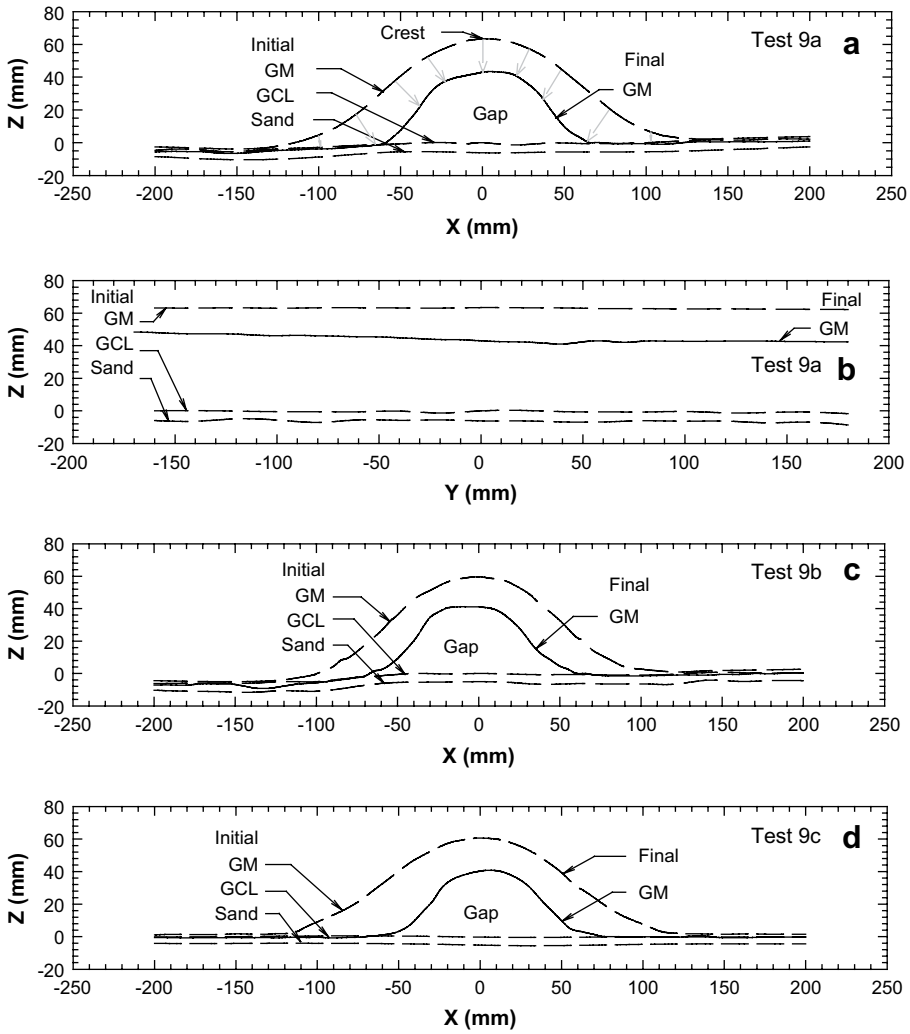

Fig. 5. Initial and final wrinkle shapes of three duplicate tests with a dry GCL beneath GM wrinkle directly backfilled with gravel and subjected to 250 kPa.

The influence of the foundation layer beneath the GCL on geomembrane strains can be assessed by comparing Test 1 with Test 8, for an initially dry GCL with no protection layer. In Test 1 with stiff sand beneath the GCL, the deformation of the geomembrane was limited to 2 mm; whereas the much softer clay subgrade in Test 8 produced indentations up to 6 mm deep resulting in a peak strain of 22% compared to 13% for Test 1 (Table 1). For reference, Gudina and Brachman (2006a) reported a geomembrane strain of 32% for with only compacted clay beneath the geomembrane and otherwise identical conditions to Test 8. This shows that the geosynthetic component of the dry GCL slightly stiffens the composite liner and reduces geomembrane strains in Test 8 relative to compacted clay alone.

3.2. Global deformation of wrinkle

The initial and final geometries of the geomembrane wrinkle at the centre of the test cell ($Y = 0$) are presented in Figs. 5–12. As illustrated in Fig. 5a, points along the wrinkle move downwards and inwards (towards the centre) when subjected to the applied vertical pressure. Consequently, the wrinkle height and width are reduced. The final wrinkle height and width from all tests are reported in Table 4. Since the initial wrinkle height varied slightly from test to test, values normalized with respect to their initial heights and widths (H_o and W_o) are also given in Table 4.

In all tests with sand as the foundation layer, there was only a small vertical settlement beside the wrinkle and little or no heave beneath the wrinkle. Consequently, the gap remained beneath the geomembrane. This differs to what Gudina and Brachman (2006a) observed with compacted clay beneath the geomembrane where the gap beneath the geomembrane wrinkle could be completely filled with clay depending on the water content of the clay and the applied pressure. There was clay heave beneath the wrinkle for the test with compacted clay as the foundation layer beneath the GCL. The gap was nearly filled with an initially dry GCL (Test 16; Fig. 12a) and completely filled with the wet GCL (Test 17; Fig. 12b). Heave of the clay foundation layer meant that the overlying GCL experienced lateral tensile elongation directly beneath the wrinkle, although there was no visual evidence of damage to the GCL in either of these tests.

The variation of wrinkle deformation along the Y-axis is depicted in Fig. 5b. While this is from Test 9a, the results from other tests have similar features in that there were no abrupt changes in the wrinkle geometry along its length resulting from either the effect of end boundary or coarse gravel backfill. To quantify the variability in the wrinkle deformation along the wrinkle crest, both the average final wrinkle height ($\overline{H}$) and width ($\overline{W}$) for 10 sections in the interval $-50 \le Y \le 50$ mm, and the final height (H) and width (W) at $Y = 0$ are given in Table 4. In all tests, the final wrinkle height and width at $Y = 0$ lie within the 95% confidence interval of the average for $-50 \le Y \le 50$ mm. Consequently, the results in Figs. 5–12 obtained at $Y = 0$ can be considered representative of the central portion of the wrinkle.

Fig. 5a, c and d compares the results of three replicate tests with a dry GCL and sand foundation layer beneath the geomembrane (Tests 9a–c) to examine the reproducibility of the results obtained from tests conducted under the same conditions. The results from these three tests are very similar, with a difference in the final wrinkle height of only 2.7 mm (for initial height difference of 2.8 mm) and no measurable difference in the final width. When normalized with respect to the initial wrinkle geometry, the results from these duplicate tests are essentially identical with $H/H_o = 69\%$ for Tests 9a and b and 67% for Test 9c and $W/W_o = 52\%$ (Table 4). The variability in final wrinkle dimensions is only slightly larger for tests with a hydrated GCL. This is attributed to the increased variability of initial GCL thickness and water content. Overall, the consistency between replicate tests suggests that the chosen boundary conditions and the experimental procedures yield consistent and reproducible results.

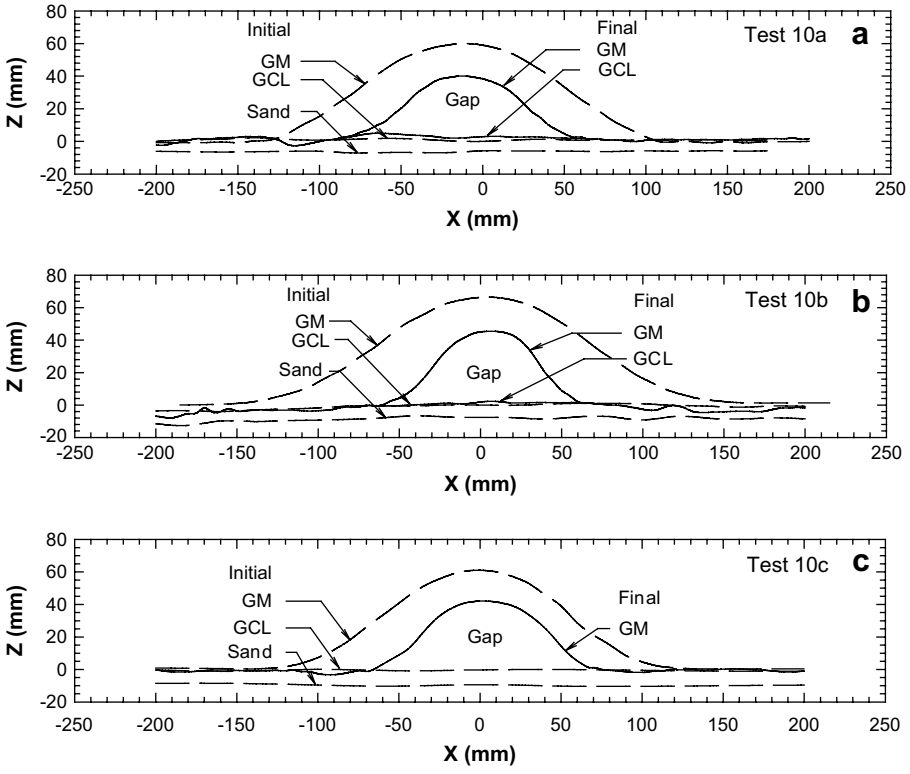

Fig. 6. Initial and final wrinkle shapes of three duplicate tests with GCL (hydrated under 20 kPa) beneath GM wrinkle directly backfilled with gravel and subjected to 250 kPa.

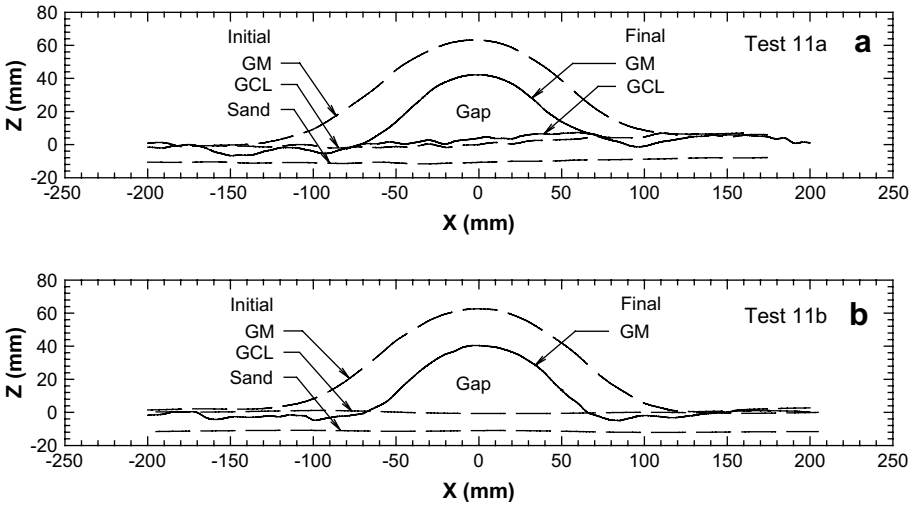

Fig. 7. Initial and final wrinkle shapes of two duplicate tests with GCL (hydrated under no confining pressure) beneath GM wrinkle directly backfilled with gravel and subjected to 250 kPa.

The effect of the initial GCL water content on the wrinkle deformations can be assessed by comparing Test 9 with Tests 10 and 11 in Tables 2 and 4. There was only a slight trend of a smaller final wrinkle height with increasing initial GCL water content, with a maximum difference in H/Ho of 5% between Tests 9a and 11b. The final wrinkle width tended to be wider for a wetter GCL with a difference of 6% in W/Wo between Tests 9 and 11. The effect of GCL water content on the wrinkle deformation was small in all the results reported here, because the displacements at the ends of the geomembrane ($X = \pm 295$ mm) were prevented; thus the potential slip due to unrestrained ends combined with the low interface friction was not permitted. Gudina and Brachman (2006b) showed that in the absence of such a restraint, geomembrane slippage (outward slip along the GM/GCL interface) as large as 16 mm (corresponding to the largest GCL water content tested) and that the final wrinkle was much smaller compared to the tests in which slippage was prevented.

The deformed shape of the wrinkle depends on the presence and type of protection layer. Comparison of Fig. 6 (Test 10) and Fig. 8 (Test 12) shows that inclusion of geotextile GT2 above the geomembrane results in a wrinkle with a similar final height but is a bit narrower. The final wrinkle was even shorter and narrower with the much heavier geotextile GT3. These differences can be explained by the differences in shear strength of the interface between the

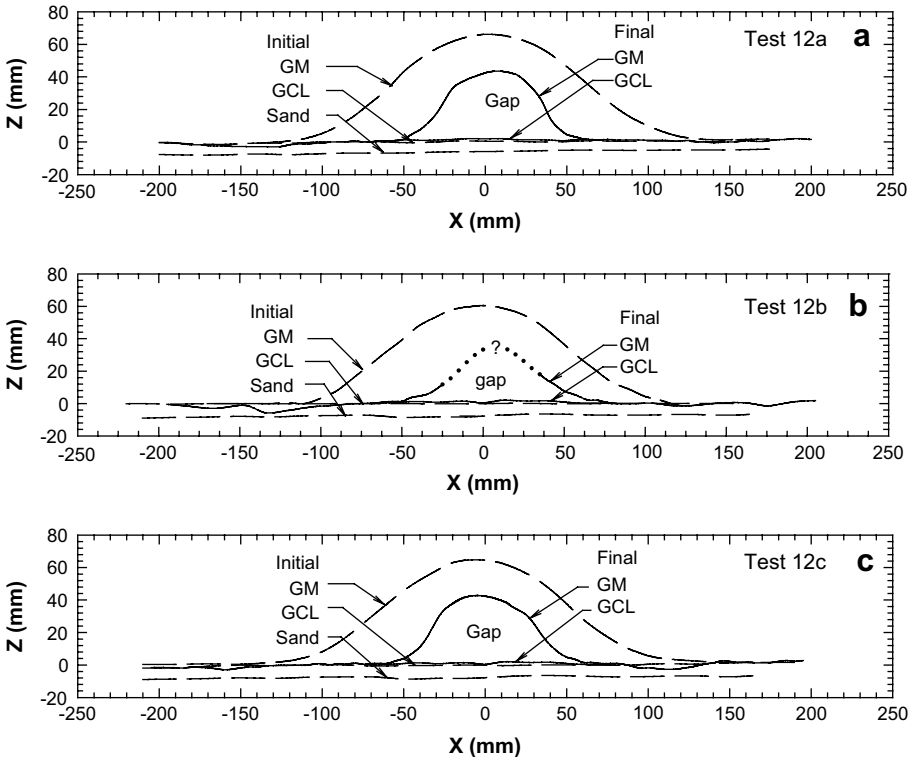

Fig. 8. Initial and final wrinkle shapes of three duplicate tests with GCL (hydrated under 20 kPa) beneath GM wrinkle with 1200 g/m^2 geotextile (GT2) protection backfilled with gravel and subjected to 250 kPa.

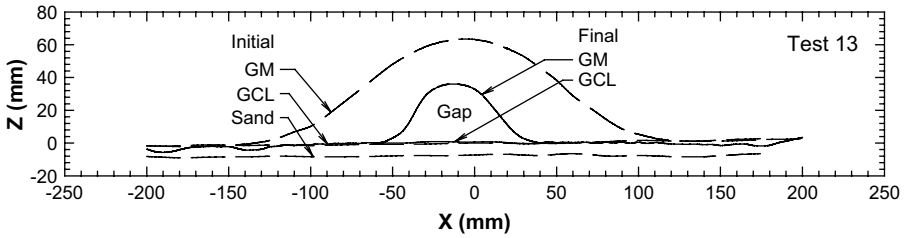

Fig. 9. Initial and final wrinkle shapes of a test with GCL (hydrated under 20 kPa) beneath GM wrinkle with 2200 g/m^2 geotextile (GT3) protection backfilled with gravel and subjected to 250 kPa.

geomembrane and the overlying material. Inclusion of GT2 reduces the interface shear strength relative to no protection (coarse gravel in direct contact with the geomembrane). This results in greater interface slip between the gravel and the geomembrane which produces a slightly narrower wrinkle in Test 12 relative to Test 10. Although the interface friction angle with a geomembrane is the same for GT3 and GT2, the contact force beneath the gravel is smaller with GT3 than GT2, since GT3 is stiffer than GT2. The result is lower interface strength with GT3, greater slip, and a shorter and narrower wrinkle in Test 13 relative to Test 12.

Out of Tests 9–13, the largest global tensile strain in the geomembrane resulting from the deformation of the wrinkle was found to be 5% (in Test 9c). This strain occurred at the side of the wrinkle ($X = 50$ mm in Fig. 5c) and was estimated from the change in geomembrane shape using membrane and bending theories treating the geomembrane as a thin cylindrical shell (Gudina, 2007). This is much smaller than the maximum geomembrane indentation strain of 14% for this configuration (Test 1 in Table 1), demonstrating that in this case local indentations govern the assessment of overall tensile strain.

Considering the results with a 150-mm-thick sand (SP) protection layer above the geomembrane (Tests 14a–c, Fig. 10), the average values of H/H_o and W/W_o of 59 and 44%, respectively, a shorter and narrower wrinkle, is obtained relative to no protection. In this case a narrower wrinkle results because greater horizontal stresses develop in the sand relative to the coarse gravel (given that the coefficient of lateral earth pressure in the sand is greater than that for the gravel tested, Brachman et al., 2001) and that the sand is able to better conform to deformed shape of the wrinkle. Global strains estimated from the deformed shape of the wrinkle showed no tension from the deformation of the wrinkle (the smallest compressive strain of 0.6% was found near the wrinkle centre).

Comparison of the results from Test 15 (conducted at 1000 kPa) with the results from Tests 14a–c (250 kPa) shows that the wrinkle becomes even smaller at higher pressures. However, the physical gap beneath geomembrane remained in Test 15. Assessment of the strains arising from the deformation of the wrinkle showed no tensile strain and greater compressive strains at 1000 kPa relative to 250 kPa.

3.3. Local strains with a wrinkle

Local indentation strains in the geomembrane from the tests with a wrinkle are reported in Table 2. These strains were also

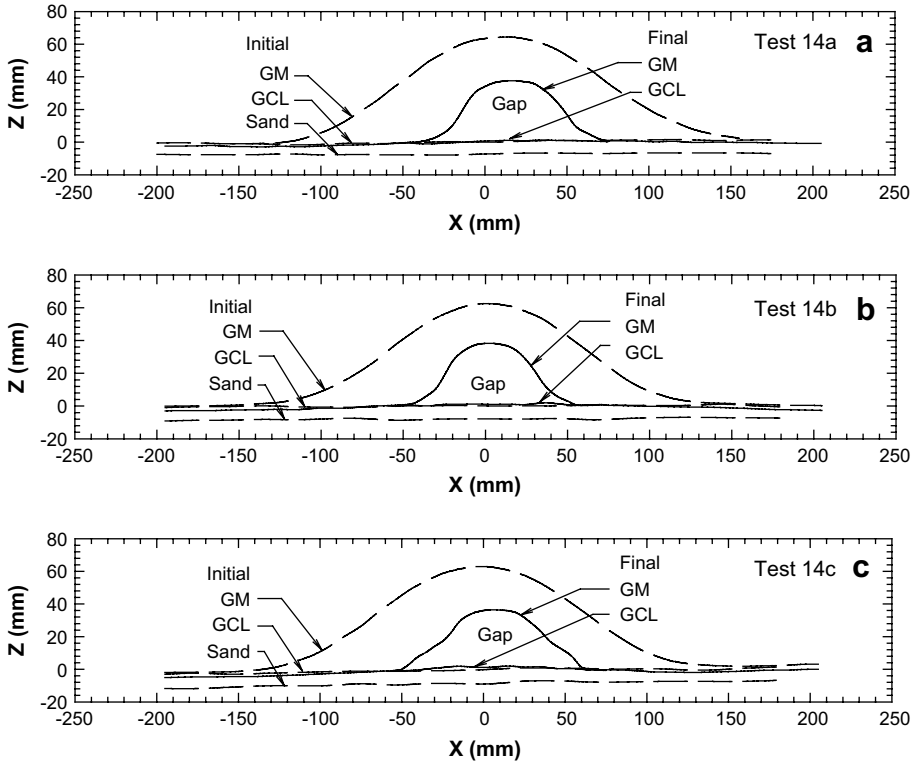

Fig. 10. Initial and final wrinkle shapes of three duplicate tests with GCL (hydrated under 20 kPa) beneath GM wrinkle (with 150-mm sand protection) backfilled with gravel and subjected to 250 kPa.

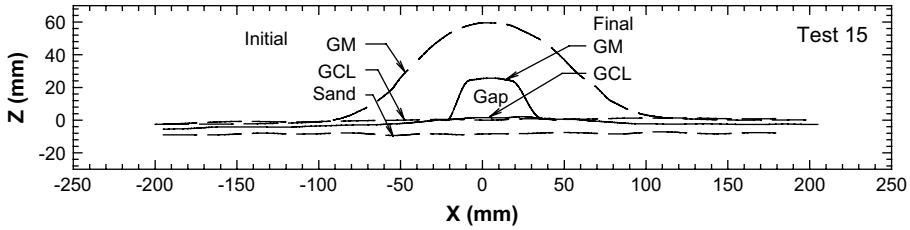

Fig. 11. Initial and final wrinkle shapes of a test with GCLch (20 kPa) beneath GM wrinkle (with 150-mm sand protection) backfilled with gravel and subjected to 1000 kPa.

calculated from measured geomembrane indentations using the procedure of Tognon et al. (2000). All of these points were initially located on the near the edge of the wrinkle, while at the end of the test they were located directly beside the deformed wrinkle (e.g., within the regions defined by $-½W_o < X < -½W$ and $½W < X < ½W_o$). For example, the deformations that can be seen in Fig. 6a–c at $X = -120$, 110 and 90 mm produced the largest tensile strain in these tests. There is a general trend of higher local geomembrane strains with a wrinkle than without, although there is not enough data to precisely quantify this effect given real variations from the 50-mm coarse gravel tested. The importance of including a wrinkle in the assessment of local geomembrane strain may be best illustrated by examining the tests with GT3 as the protection layer. Recalling for comparison that without a wrinkle the strains with GT3 were just below one limit of 6% (Test 6, Table 1), the strains increased to 7.5% when a wrinkle was tested (Test 13, Table 2). The local geomembrane strains are believed to be larger with a wrinkle because of the redistribution of vertical stresses above the wrinkle to either side of the wrinkle, thus leading to larger contact forces beside the wrinkle. However, the 150-mm-thick sand protection was effective in reducing the local geomembrane strain even in the presence of a wrinkle (Test 14, Table 2), limiting the local geomembrane strain to less than 0.3%.

The increases in local strain due to a wrinkle overlying a GCL and firm sand foundation layer were found to be smaller than that reported by Gudina and Brachman (2006a) for compacted clay beneath the geomembrane. They reported that the local strain increased from 32% for flat geomembrane to 42% for a geomembrane with a wrinkle (both with no protection layer). The effect of a wrinkle on local strains is less because of less arching arising from smaller vertical settlements on either side of the wrinkle of the stiff sand foundation soil relative to the softer compacted clay layer.

4. Conclusions

Strains and deformations of a 1.5-mm-thick, high-density polyethylene geomembrane (GM) when placed on top of a geosynthetic clay liner (GCL), buried beneath 50-mm coarse gravel and subjected to vertical pressure were reported. For the specific materials (50-mm coarse gravel backfill, protection layers, 1.5-mm-thick high-density polyethylene GM, needle-punched GCL and subgrades) and conditions tested at a vertical pressure of 250 kPa, the main conclusions are:

(1) Local strains: the local geomembrane strains caused by indentations from the overlying gravel were found to increase with increases in initial GCL water content, with decreases in the stiffness of the foundation layer, and by the presence of a wrinkle. The maximum tensile strains in the geomembrane occurred directly beside the deformed wrinkle.
(2) Protection layers: the local geomembrane strains were reduced by increasing the mass per unit area of a nonwoven needle-punched geotextile protection layer. However, none of the geotextiles tested (with masses up to 2200 g/m^2) were able to limit tensile strains of the geomembrane to proposed allowable limits (3 or 6%). A 150-mm-thick layer of sand between the gravel and geomembrane was able to limit local tensile strains in the geomembrane to less than 0.3%.
(3) Wrinkle deformations: the wrinkle decreased its height and width when subjected to vertical pressure. The physical gap between the geomembrane and GCL beneath the wrinkle was reduced, but remained, when the GCL was underlain by the firm sand foundation layer. The gap was eliminated with the softer clay foundation layer. The deformed shape of the wrinkle depended on the type of protection layer, the applied vertical pressure, and the water content of the GCL. It

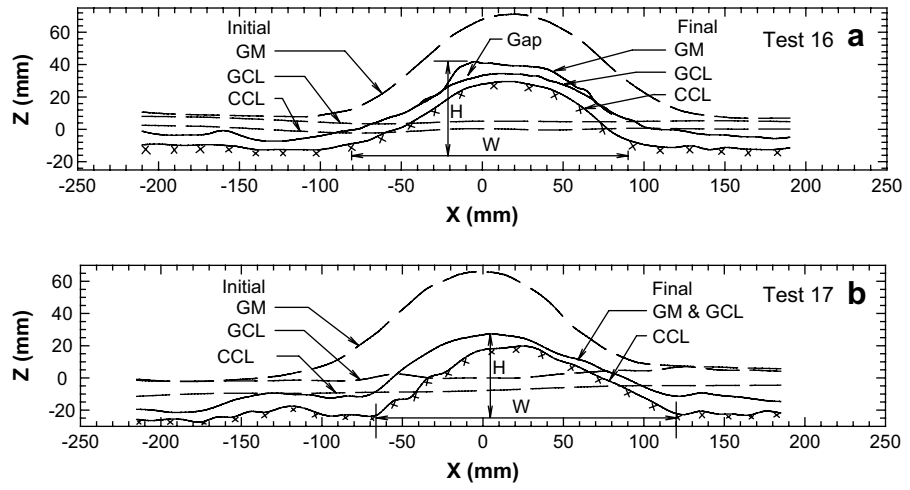

Fig. 12. Initial and final shapes of a geomembrane wrinkle backfilled directly with gravel and subjected to 250 kPa with: (a) dry GCL and (b) hydrated GCL (with zero confining pressure) beneath GM wrinkle.

Table 4
Final wrinkle geometry

Test	Average over $-50 < Y < 50$ mm				At $Y = 0$			
	$\overline{H}$ (mm)	±95% CI (mm)	$\overline{W}$ (mm)	±95% CI (mm)	H (mm)	H/H_o (%)	W (mm)	W/W_o (%)
9a	43.4	0.8	126	2.0	43.5	69	125	52
9b	41.0	0.6	126	1.2	41.0	69	125	52
9c	40.9	0.5	128	2.0	40.8	67	125	52
10a	39.5	0.6	135	5.2	40.0	66	130	54
10b	44.9	0.4	120	0	45.2	68	120	50
10c	42.2	0.4	134	4.8	42.1	67	130	54
11a	41.8	0.2	132	2.4	42.0	67	140	58
11b	39.0	0.6	138	3.9	40.0	64	140	58
12a	43.2	0.2	112	1.4	43.4	66	110	46
12b	–	–	114	3.5	–		115	48
12c	43.4	1.9	122	3.0	42.8	67	115	48
13	35.3	0.3	95	2.1	35.6	57	95	40
14a	37.4	0.2	107	1.5	37.6	58	105	44
14b	37.9	0.4	103	1.5	38.2	61	100	42
14c	36.0	0.4	100	3.7	36.4	59	110	46
14d	42.5	0.2	108	2.4	42.7	63	105	44
15	25.3	0.4	55	0.9	25.7	43	55	23
16	–	–	190	5.0	42.9	67	170	71
17	–	–	195	5.0	50.0	76	185	77

$\overline{H}$ and $\overline{W}$ are the average height and width of the deformed wrinkle, respectively. Y is the distance from the centre of the test cell.

was found that tensile strains in the geomembrane could also result from deformation of the wrinkle. However, these tensile strains were smaller than the local strains from gravel indentations; consequently, the local indentations would govern the assessment of overall tensile strain in the geomembrane. In the case of the sand protection layer, no tension was calculated from the wrinkle deformations because of greater wrinkle deformations (even in one test up to 1000 kPa).

(4) Practical implications: the results reported in this paper show that nonwoven needle-punched geotextiles selected solely to prevent puncture and with masses up to 2240 g/m^2 are insufficient to limit tensile strains below 3% in the high-density polyethylene geomembrane tested, for the case of nominal 50 mm coarse, angular, poorly graded gravel above the geomembrane and then subjected to a vertical pressure of 250 kPa; whereas a 150-mm-thick sand protection layer was able to limit the tensile strain to less than 1%.

The reported deformations and strains are expected to underestimate those expected at the base of a landfill since they were obtained from short-term tests conducted at 22 °C and without chemical exposure. Work is currently under way to quantify the combined effects of applied stress, elevated temperature and chemical exposure on geomembrane strains and deformations.

Acknowledgements

Funding was provided by the Natural Sciences and Engineering Research Council of Canada, the Canadian Foundation for Innovation and the Ontario Innovation Trust. S. Dickinson assisted with the experiments. The geomembrane was provided by Solmax International, the GCL by Terrafix Geosynthetics, and the geotextile protection layers by Naue Fasertechnik, Huesker Synthetic and Terrafix Geosynthetics.

References

ASTM. 1992. Standard practice for determination of 2% secant modulus for polyethylene geomembranes. ASTM D 5323, West Conshohocken, PA, pp. 133–135.
ASTM. 2001. Standard test method for determining tensile properties of nonreinforced polyethylene and nonreinforced flexible polypropylene geomembranes. ASTM D 6693, West Conshohocken, PA, pp. 392–395.
Barroso, M., Touze-Foltz, N., von Maubeuge, K., Pierson, P., 2006. Laboratory investigation of flow rate through composite liners consisting of a geomembrane, a GCL and a soil liner, 24 (3), pp. 139–155.
Benson, C.H., Daniel, D.E., Boutwell, G.P., 1999. Field performance of compacted clay liners. Journal of Geotechnical and Geoenvironmental Engineering – ASCE 125 (5), 390–403.
Bouazza, A., Vangpaisal, T., 2006. Laboratory investigation of gas leakage rate through a GM/GCL composite liner due to a circular defect in the geomembrane. Geotextiles and Geomembranes 24 (2), 110–115.
Bouazza, A., Vangpaisal, T., Abuel-Naga, H., Kodikara, J., 2008. Analytical modelling of gas leakage rate through a geosynthetic clay liner–geomembrane composite liner due to a circular defect in the geomembrane. Geotextiles and Geomembrane 26, (2), 122–129. (on the web – Elsevier please complete since issue and page numbers should be known at time of type setting).
Brachman, R.W.I., Moore, I.D., Rowe, R.K., 2001. The performance of a laboratory facility for evaluating the structural response small diameter buried pipes. Canadian Geotechnical Journal 38 (2), 260–275.
Brachman, R.W.I., Gudina, S., 2002. A new laboratory apparatus for testing geomembranes under large earth pressures. In: Proceedings of the 55th Canadian Geotechnical Conference, pp. 993–1000.
Dickinson, S., Brachman, R.W.I., 2006. Deformations of a geosynthetic clay liner beneath a geomembrane wrinkle and coarse gravel. Geotextiles and Geomembranes 24 (5), 285–298.
Fleming, I.R., Rowe, R.K., 2004. Laboratory studies of clogging of landfill leachate collection and drainage systems. Canadian Geotechnical Journal 41 (1), 134–153.
Fox, P.J., DeBattista, D.J., Mast, D.G., 2000. Hydraulic performance of geosynthetic clay liners under gravel cover soils. Geotextiles and Geomembranes 18, 179–201.
Gudina, S., 2007. Short-term Physical Response of HDPE Geomembranes from Gravel Indentations and Wrinkles. PhD thesis, Queen's University, Kingston, Canada.
Gudina, S., Brachman, R.W.I., 2006a. Physical response of geomembrane wrinkles overlying compacted clay. Journal of Geotechnical and Geoenvironmental Engineering – ASCE 132 (10), 1346–1353.
Gudina, S., Brachman, R.W.I., 2006b. Effect of boundary conditions on deflection of geomembrane wrinkles in a GM/GCL composite liner. In: Proceedings of Eighth International Conference on Geosynthetics, Yokohama, Japan (CD-Rom).
Koerner, R.M., Wilson-Fahmy, R.F., Narejo, D., 1996. Puncture protection of geomembranes Part III: examples. Geosynthetics International 3 (5), 655–675.
MOE, 1998. Landfill Standards: a Guideline on the Regulatory and Approval Requirements for the New or Expanding Landfilling Sites, Ontario Ministry of the Environment, Ontario Regulations 232/98. Queen's Printer for Ontario, Toronto.
Peggs, I.D., Schmucker, B., Carey, P., 2005. Assessment of maximum allowable strains in polyethylene and polypropylene geomembranes. In: Proceedings of ASCE Geo-Frontiers 2005, Austin, TX (CD-Rom).
Pelte, T., Pierson, P., Gourc, J.P., 1994. Thermal analysis of geomembrane exposed to solar radiation. Geosynthetics International 1 (1), 21–44.
Rowe, R.K., 2005. Long-term performance of contaminant barrier systems. 45th Rankine Lecture. Geotechnique 55 (9), 631–678.
Rowe, R.K., Quigley, R.M., Brachman, R.W.I., Booker, J.R., 2004. Barrier Systems for Waste Disposal Facilities. Taylor & Francis Books Ltd. (E & FN Spon), London, 587 pp.
Rowe, R.K., Mukunoki, T., Bathurst, R.J., Rimal, S., Hurst, P., Hansen, S., 2007. Performance of a geocomposite liner for containing Jet A-1 spill in an extreme environment. Geotextiles and Geomembranes 25 (2), 68–77.
Saidi, F., Touze-Foltz, N., Goblet, P., 2008. Numerical modelling of advective flow through composite liners in case of two interacting adjacent square defects in the geomembrane. Geotextiles and Geomembranes 26 (2), 196–204. on the web – Elsevier please complete since issue and page numbers should be known at time of type setting.
Seeger, S., Müller, W., 2003. Theoretical approach to designing protection: selecting a geomembrane strain criterion. In: Dixon, D., Smith, D.M., Greenwood, J.R., Jones, D.R.V. (Eds.), Geosynthetics: Protecting the Environment. Thomas Telford, London, pp. 137–151.
Soong, T.-Y., Koerner, R.M., 1998. Laboratory study of high density polyethylene geomembrane waves. In: Proceedings of Sixth International Conference on Geosynthetics, vol. 1. Industrial Fabrics Association International, Atlanta. 301–306.
Tognon, A.R., Rowe, R.K., Brachman, R.W.I., 1999. Evaluation of side wall friction for a buried pipe testing facility. Geotextiles and Geomembranes 17 (4), 193–212.
Tognon, A.R., Rowe, R.K., Moore, I.D., 2000. Geomembrane strain observed in large-scale testing of protection layers. Journal of Geotechnical and Geoenvironmental Engineering – ASCE 126 (12), 1194–1208.
Touze-Foltz, N., Duquennoi, C., Gaget, E., 2006. Hydraulic and mechanical behavior of GCLs in contact with leachate as part of a composite liner. Geotextiles and Geomembranes 24 (3), 188–197.